SSD - a Silicon Strip Detector for STAR

Barbara Erazmus, Hans Gutbrod, Lilian Martin
SUBATECH, Nantes, France

Jean-Pierre Coffin, Christian Kuhn
CNRS, Strasbourg, France

Rene Bellwied, Claude Pruneau, Ken Wilson
Physics Department, Wayne State University, Detroit

ABSTRACT

We propose to build a Silicon Strip Detector barrel for STAR. The main components will be wafers, support and electronics designed for the ALICE strip detector.

1. Design

We propose to build a single barrel of double sided Silicon strip detectors to be integrated into STAR as an additional tracking detector between the SVT and the TPC. The detectors foreseen for this layer are the detectors currently developed for the two outer layers of the inner tracker of ALICE [1]. The strip detectors have a thickness of 300 micron, and a size of 4.2 cm by 7.5 cm. The detectors will be produced on 4-inch wafers and a conservative dead area of 1 mm total width along both dimensions is assumed for the guard ring, the bias line, the readout pads. The bonding of the bottom side strips to the pre-amplifier glued to the top side of the wafer, requires an additional 1 mm spacing between detectors. This leads to a geometrical hardware efficiency of 94%. The strips will be 4.1 cm long and oriented parallel to the beam axis. The geometrical hardware efficiency will be improved by tiling the detectors in the bending plane. Each ladder will be slightly tilted allowing each detector to overlap with the detectors on the neighboring ladders. In these conditions, the geometrical hardware efficiency of the SSD layer will reach 95%.

The stereo angle between the top and bottom side of the wafers is 35 mrad. Each side has 768 strips with a strip pitch of 96 micron which leads to 1536 channels per wafer.

The strip pitch and the stereo angle values are the results of a compromise between the position resolution and the number of ambiguous hits. The average single strip occupancy expected for $Au+Au$ collisions at RHIC is 0.6% ($.16 hits/cm^2$ at $r = 25cm$, 5 hits/det.) whereas the probability to have ambiguous hits will be smaller than 10%

(defined as the width of a strip times the number of stereo strips crossing). With the strips parallel to the beam axis and a pitch of $96\mu m$ a resolution of the the order of $25-30\mu m$ and $800-900\mu m$ can be reached respectively in the bending plan and the beam direction. The matching of the charges collected on the two sides of a detectors will be used to resolve ambiguous hits. With the signal to noise ratio expected for the detector (see the section on the front-end electronics) a detector efficiency better than 95% should be reached. Moreover, the small stereo angle allows to readout the signal strips of both sides on a single edge of the detector, thus avoiding extra passive layers needed to re-route strips.

Our simulations suggest that the barrel should be placed at a radius of 25.38 cm. The detector consists of 22 ladders with 16 wafers each to cover $\eta\pm1\pm4$ cm, which exceeds slightly the SVT coverage. A total of 352 detectors leads to 540,672 channels. Fig.1 shows a three dimensional view of the SVT including the SSD. Fig.2 shows an endcap view of the proposed SSD implementation.

The following table resumes the basic characteristics of the layer :

detector size	$7.5 \times 4.2cm^2$
active area	$7.4 \times 4.1cm^2$
strip pitch	$96\mu m$
stereo angle	$35mrad$
number of strips/det.	2×768
number of ladder	22
detectors per ladder	16
total number of detectors	352
total number of channels	540,672
total area	$1.135m^2$

On the top of each detector 12 preamplifier/shaper chips will be glued directly to the Silicon. Each chip reads out 128 channels. The signals are transfered via a Kapton cable to the ends of the support ladder, where ADC boards will be located. The signals are multiplexed (1536:1), so that each wafer is served by one ADC. Digital signals will then be driven along the SVT cone to the SVT readout electronics area (1 cable per detector = 352 cables). The electronics is detailed in the following section.

The original ALICE support structure will be adapted for the layer. The structure is made of carbon-fiber and has a triangular shape with the detectors glued to the top side of the triangle (see fig.3). Carbon fiber was chosen based on its rigidity and light weight. The proposed structure is made of three carbon tubes attached together with the help of 22 sets of three smaller carbon tubes forming a triangle with 3.6 cm edges. Each ladder will support 16 detectors and 2 ADC boards. The overall length of the active area is exactly 68.8 cm (16 $\times$4.2 cm + 1 mm spacing between wafers). We reserved 10 cm on each side for the ADC board plus a 6 mm spacing between the Silicon detectors and the ADC boards, which leads to a total length of 90 cm for the structure.

We suggest to support the structure from the SVT water manifold which covers the range from 34 to 50 cm from the vertex in z-direction, respectively. The Carbon support tubes will be screwed into a Carbon fiber water manifold which also serves as an endring for the SSD. This manifold is then supported off the SVT water manifold via 10 Aluminum tubes (0.25 inches inner diameter, height = 5.32 cm). These standoffs are screwed into a boss with a tapped hole that was welded to the outer surface of the SVT manifold in locations between the SVT transition boards.

The SSD endring/water manifold is a clam-shell structure which opens at the 3 and 9 o'clock position, so that the two half shells can be removed without interfering with the SVT installation beams and the beam pipe. The SVT halves open towards the 3 and 9 o'clock position to not interfere with the Beryllium rods that connect the SVT support cones. The SSD is mounted at a larger radius than the Beryllium rods. When the SSD is in place it will define the outer radius of the inner tracker. Therefore the aluminized mylar grounding sheet for the SVT will be wrapped around the SSD rather than the 3rd layer of the SVT.

The overall weight of the SSD including structure, wafers, cooling, electronics and cables is estimated to be below 20 lbs.

2. Cooling

The SSD requires water cooling for the frontend electronics, glued to the wafer surface and the ADC ear boards. Two carbon pipes, running along the structure axis, will be attached to evacuate the heat produced. The frontend electronics is mounted on a heat bridge which connects the two cooling tubes. The 44 water tubes (0.1 cm inner radius) connect directly to the SSD water manifold/endring structure. The power consumption of the electronics is about 1.4 mW/channel (1 mW/ch. from the frontend and 0.4 mW/ch. from the ADC), which leads to an overall heat dissipation of 746 W on the surface of the SSD, less than the SVT-FEE power consumption of 1350 W (about 13 mW/channel). We therefore suggest that the SSD water is supplied by the SVT water manifold. The SVT engineers suggest to branch off ten SSD input lines from the ten SVT water hoses running down the support pipe to connect to the SVT water manifold. These 10 SSD input lines will then be fanned out to 44 output lines at the SSD endring.

The electronics will be held to room temperature (75 degree Fahrenheit). There will be little heat dissipation from the detectors or electronics to the ambient air. We expect no effect on the air temperature for the SVT and TPC volumes.

3. Electronics

The data will be read out by a custom made CMOS preamplifier shaper (PASA) to be developed by the group in Strasbourg for ALICE. The preamplifier has 128 channels and a shaping time of 800 ns. That requires a trigger to be delivered to the system within 1 μs. Presently STAR delivers a 2μs trigger, which might have to lead to a re-design of the PASA.

Each channel of the chip will treat the signal induced on the strip in three distinct stages : pre-amplification, shaping, sampling and holding and eventually in a 4th level a discrimination. In addition, the output signals will be multiplexed to a single signal per chip and further multiplexed to a single cable per detector to reach a multiplexing rate of 1536:1. The relatively long shaping time allows to avoid the use of analog delays or analog switch capacitors to match the trigger arrival time. However, this solution limits the running rate of the layer to avoid pile-up in the silicon detectors. According to ALICE requirements for their silicon strip detector electronics and assuming that we will use the same chip, a low noise level below 400 electron equivalent noise can be reached leading to a signal to noise ratio of 60 for minimum ionizing particles. One should keep in mind that the charge matching algorithm to resolve ambiguities relies strongly on a high S/N ratio. The power consumption should be low enough to limit the heat to 1 mW per channel. The detector and the associated front-end electronics will require several control and bias signals :

designations	numbers
output signal	1
low voltages	3 ?
high voltages	1
clock signal	1
discri. threshold	1
discri. multiplicity	1
test signals	3
trigger signal	1

Detectors will be powered with a single 100 V line, which is daisy-chained across the ladder. There will be three low voltage lines to supply the operating voltage for the frontend. They will be daisy-chained as well.

The data from a single wafer are multiplexed into one signal line on a aluminized polyamide cable of 12 μm thickness per cable layer. This cable is connected to ADC boards at the ends of each ladder. Each ADC board holds 8 ADCs to serve 8 wafers. The 1536 analog channels from one detector will be digitized (at 10 MHz) by a commercial 10-bit flash ADC. The read frequency for the ADC is 666 Khz (1.5 μs). From the ADCs the digitized data are driven to the SVT readout electronics area at the TPC wheel. The cables are identical to the SVT cables running along the SVT cone. In the SVT readout area each SSD ladder will be served by one SVT power-timing board (PTB) and one SVT fiber optic board (FOB). That means the SSD will add 2 boards to 22 of the 24 SVT readout sectors.

High voltage, low voltage, and pulser signals for the SSD will be generated in the SVT rack space on the STAR platforms.

4. Data volume and processing

The data volume on each FOB is about 98 KByte (16 wafers × 1536 channels × 32 bits (10 bit ADC and 22 bits addresses)). The overall unsurpressed data volume is 2.16 MByte.

Zero suppression will be performed by the SVT-ASICs. The ASIC boards are located in the DAQ racks in the STAR counting house, which leads to a fiber link length of about 50-100 m. Simulations show that a 2% occupancy in the detector is realistic. Therefore the total SSD data volume after suppression is 43 KByte per event.

The detector could provide a trigger for level 3 based on the discrimination capabilities of the frontend chips. To simplify the STAR event builder we do not propose this option at this point. Therefore the SSD data can be processed to tape in the same fashion than the SVT data.

5. Radiation length

The following values are based on the estimates made for the ALICE technical proposal. although prototypes of the preamplifier and the carbon ladder exist, the electronics as well as the support structure are still in the conceptual stages. Therefore these number have to be considered preliminary. All numbers are average numbers for the complete structure. There are no identifiable locations of serious radiation length enhancement in the design, though. Every source of radiation length is evenly distributed across the ladders.

The following components will contribute to the SSD radiation length.

wafers	0.32%
electronics	0.05%
capton cables	0.03%
support (incl. cooling tubes, heat bridges)	0.2%
mylar grounding shield	0.05%
total average	**0.65%**

In addition we expect the endrings to contribute around 2% radiation length at around η=1.6, respectively.

6. Physics justification

The physics justification for a intermediate tracking detector between the SVT and the TPC is established by investigating three different components of the tracking in STAR, namely the improvement to the tracking performance, the improvement to existing STAR physics observables and the possibility of new physics observables.

This proposal will extend the scope of the study of a fourth layer for the SVT, which was published last year (STAR note 232 [2]). To perform these studies we implemented the design as described in the previous sections into GSTAR, the STAR-GEANT simulation package. Figs.1, 2, and 3 are outputs of the GEANT package.

6.1. Improvements to the existing STAR tracking system performance

a.)Redundancy and SVT tracking efficiency

The main advantage of an additional Silicon layer close to the SVT is that the number of spacepoints on a primary SVT track is increased from four to five (including the vertex). Therefore the present hardware inefficiency of the SVT (18% due to 6.5% guard area per SVT layer) will be fully recovered by simply using the additional SSD information and keeping the existing tracking software, but allowing a missing spacepoint on the track. Primary and secondary tracking efficiencies will increase accordingly.

b.) Enhanced matching efficiency

The SSD will provide a well defined space point about halfway between the SVT and the TPC, at exactly the location where the present SVT-TPC matching code defines an imaginary plane to merge the tracks. An additional space point with good position resolution will greatly enhance the vector-to-vector matching efficiency. The matching plane could be moved in between the SSD and the TPC (at about 37 cm radius).

In addition, the SSD allows to explore the possibility of TPC vector to SSD spacepoint matching. The improvement in the search area, comparing the projected TPC resolution and the actual SSD resolution (20 μm by 800 μm), is about a factor five.

Both effects should improve the overall STAR matching efficiency to better than 90%. Detailed studies are under way.

c.) Increased SVT momentum resolution

The SVT standalone momentum resolution will improve greatly for particles of all momenta. Fig.4 shows a comparison between the existing three layer tracker and the proposed four layer device. For secondaries (no primary vertex reconstruction), the resolution improves from a marginal 25% at low momentum to about 12%. The standalone resolution for primaries improves from 16% to 10%.

Fig.5 shows that the degradation in the TPC momentum due to the additional layer is negligible.

d.) Improved particle identification capability

The SSD adds another 300 micron Silicon layer to the SVT, which translates into an additional dE/dx measurement for low momentum tracks. The dE/dx resolution will improve accordingly.

e.) Improvement in $c\tau$ acceptance for short-lived particles

Adding a fourth layer to the inner tracker in STAR leads to a better $c\tau$ acceptance for decay particles. The requirement for a primary decay can be relaxed to a maximum distance from the primary which corresponds to the radius of the second layer of the SVT (r=10.6 cm) rather than the first layer (6.63 cm). The cut on the primary vertex (distance of closest approach) remains unchanged. To document this improvement in reconstruction efficiency we calculated the increased number of reconstructed decays for Λ and Ξ particles.

The numbers quoted in the following include the improvement due to the increase $c\tau$ cut and the increased hardware efficiency.

The detection efficiency for Λ particles improves from 58% to 85%.

The detection efficiency for Ξ particles improves from 26% to 53%. The effect on the Ξ is more dramatic due its shorter lifetime. To generate the final tracker reconstruction efficiency, these detection efficiencies have to be folded with various other cuts. The following section shows an example for the overall Λ reconstruction.

f.) Possible level 3 trigger

The strip detector will be able to provide charged particle multiplicity information to a level 1 trigger. Its readout time is about 1 μs. The pixelation of the device (96 μm by 800 μm) is superior to other STAR detectors that measure multiplicity as well (CTB and TPC).

Charged particle multiplicity can be used as a standard centrality trigger or as a physics trigger (e.g. event topology) if measured with sufficient segmentation. The SSD provides the necessary accuracy.

6.2. Improvements to STAR physics observables

a.) Effects on strange and multi-strange baryon/antibaryon reconstruction

In the following we choose the Λ particle reconstruction as an example for the improved tracking performance of STAR. Table 1 compares the original STAR efficiencies [3] to efficiencies including the SSD for a Λ sample in the pseudo-rapidity coverage of the SVT. For the comparison we treat the SSD as a fourth layer of the SVT.

Parameter	SVT+TPC	SVT+SSD+TPC
Branching ratio	0.642	0.642
TPC secondary tracking efficiency	$0.8^2 = 0.64$	$0.8^2 = 0.64$
SVT secondary tracking efficiency	$0.7^2 = 0.49$	$0.9^2 = 0.81$
SVT-TPC matching efficiency	$0.85^2 = 0.73$	$0.9^2 = 0.81$
Cτ acceptance (incl. SVT hardware efficiency)	0.58	0.85
V0 finding efficiency (incl. vertex cut)	0.67	0.67
Total reconstruction efficiency	0.06	0.15

Analytical calculations show that the improvement for multi-strange baryons is even larger due to the enhanced $c\tau$-acceptance.

b.) Effect on HBT studies

Based on the calculations shown in the SVT proposal to the DoE [4], we concluded that the SVT will contribute in two major categories to the STAR-HBT capabilities: (1) by extending the acceptance to low $p_{\perp}$ and (2) by enabling neutral kaon (K_s^0) interferometry.

The addition of the SSD in the current SVT geometry will have a significant effect on the STAR capabilities to do interferometry measurement. So far, the SVT does not have the momentum resolution to do HBT in a stand-alone mode and the use of the TPC tracks requires a low momentum cut which results in poor statistics at low relative momentum. The SSD layer will provide a better momentum resolution at low p_t and the enhanced reconstruction efficiency will increase the size of the samples used for calculating correlation functions. Up to a factor of three in the number of pairs can be expected in the low momentum region if the SVT momentum resolution compares with the TPC resolution. Below 200 MeV/c the TPC resolution degrades to around 10 MeV/c, whereas the combination of SVT/SSD improves the SVT stand-alone resolution to about 15 MeV/c.

The most important improvement will be in the two-track resolution, though. Currently, the SVT two-track resolution is an order of magnitude better than the TPC resolution [4]. Fig.6 shows the effect on the uncertainty in rms radius for inclusive pion pair spectra as a function of lower momentum cutoff and two track separation in SVT and TPC. The fourth layer will have equivalent two-track separation capabilities compared to the SVT layers. Consequently, considering the larger track length due to the SSD, a much better overall two-track resolution and two-particle momentum resolution will be reached.

To summarize, with the addition of the SSD, larger and better quality samples of pairs will be accessible for particle interferometry and will lead to an extended sensitivity for larger source sizes. This is of special importance for the determination of two-pion correlation functions on an event by event base. In addition, other particle type correlation functions will be enriched and thus will support stronger cuts on different global observables (see the following section on new physics).

The K_s^0 reconstruction efficiency will be enhanced according to the improved efficiencies as quoted for strange particle decays in the preceding sections. The original SVT simulation showed that we will be able to reconstruct 2.5 K_s^0 pairs per event. The addition of an SSD will lead to a reconstruction efficiency of 7 pairs per event.

c.) Effect on low momentum particle reconstruction

The SVT standalone tracking performance at the lowest momenta (50-200 MeV/c) will be greatly improved by a fourth layer. Presently the most difficult problem in low momentum tracking is the relative enhancement of ghost tracks in the lowest momentum bins compared to the number of actual reconstructed tracks. The ghost track contamination is due to the rather large search areas used in the present tracking programs at low momenta. In those areas the double hit occupancy is enhanced over the average detector occupancy. A fourth spacepoint requirement at a larger radius will decrease the search area size. We therefore expect improvements in the determination of the pion spectral shape and their mean momentum. Both parameters might help to prove the formation of a domains of disoriented chiral condensate. Detailed studies of this effect are under way.

d.) Effect on particle flow measurement

Particle flow and entropy measurements require the reconstruction of very low momentum baryons (p,d etc.). The SSD allows a better reconstruction of low momentum baryons, due to the more constraint track fit.

6.3. New Physics

a.) $\Lambda\Lambda$-interferometry

Due to the enhanced reconstruction efficiency of strange particles, the addition of a SSD opens up the possibility of measuring Λ-pairs in an event. Before the inclusion of a fourth Silicon layer the efficiency lead to about 0.5-1 reconstructed Λ per event. In the preceeding section we show that the fourth layer will enhance the Λ yield per event by about a factor three. The number of reconstructed Λ pairs is then comparable to the number of K^0-pairs per event in the original design. Assuming a 1 Hz event rate and 5 Million reconstructed pairs to obtain a good limit on a 10 fm source size (based on the STAR K_s^0 interferometry study), we show the required running time as a function of the Λ reconstruction efficiency in Fig.8. Based on the improvement in Λ reconstruction efficiency, we can expect to obtain a statistically significant sample within six months of STAR running. More detailed studies of our interferometry efficiencies are under way.

b.) Standalone secondary tracking with the SVT

With the inclusion of a fourth layer the SVT will be capable to reconstruct low momentum strange and multistrange baryons. Therefore the phase space of decay particle reconstruction in STAR can be extended down to 50 MeV/c. Low momentum effects in strange baryon spectra can be measured by the SVT-SSD tracking system. Detailed studies of this effect are under way.

c.) Event by event non-identical particle correlations

With the current STAR design and tracking software, of the order of 600 π^+, 100 K^+ and 50 protons plus the same number of negative charged particles per $Au + Au$ collision will be reconstructed. Thus far, only same sign two-pion interferometry has been investigated in STAR. The improvement of the reconstruction efficiency (especially at low p_t) provided by the SSD will increase the sample size of all species allowing us to look at unlike-particle correlation functions event by event. The $\pi^+\pi^-$ interferometry will be feasible based on the number of reconstructed pairs (at least 360000 pairs) and all possible systems involving a pion and a kaon could be investigated (around 60000 πK pairs). However, the small number of protons produced does not allow to build the proton-pion or proton-kaon correlation functions for each event. One should note that unlike-particle interferometry is not sensitive to the two-track separation (opposite-charge particles bend in opposite directions and unlike-mass particles require totaly different particle momenta to form a low relative momentum pair).

Identical-particle interferometry provides only information on the relative space-time distances between the particle emission points. The correlation functions of non-identical particles will allow us to extract absolute values of the possible time difference or delay between the emission of different particle species [5]. This new technique, requiring only one cut in the pair phase space, will provide a unique way to study the history of a specific event (or at least a class of events) in terms of emission order for all different emitted species.

7. References

[1] ALICE Technical Proposal, CERN Report, Jan. 1996

[2] K. Wilson, STAR note 232, Nov. 1995

[3] K. Wilson for the SVT collaboration, *Proc. Quark Matter Preconf. Workshop* **UCRL-ID-121571**, 55 (1995)

[4] R. Bellwied et al., Proposal to the DoE, WSU note, Nov. 1994

[5] R.Lednicky, V.L. Lyuboshitz, B. Erazmus and D. Nouais, *Phys. Lett.* **B373**, 35 (1996)

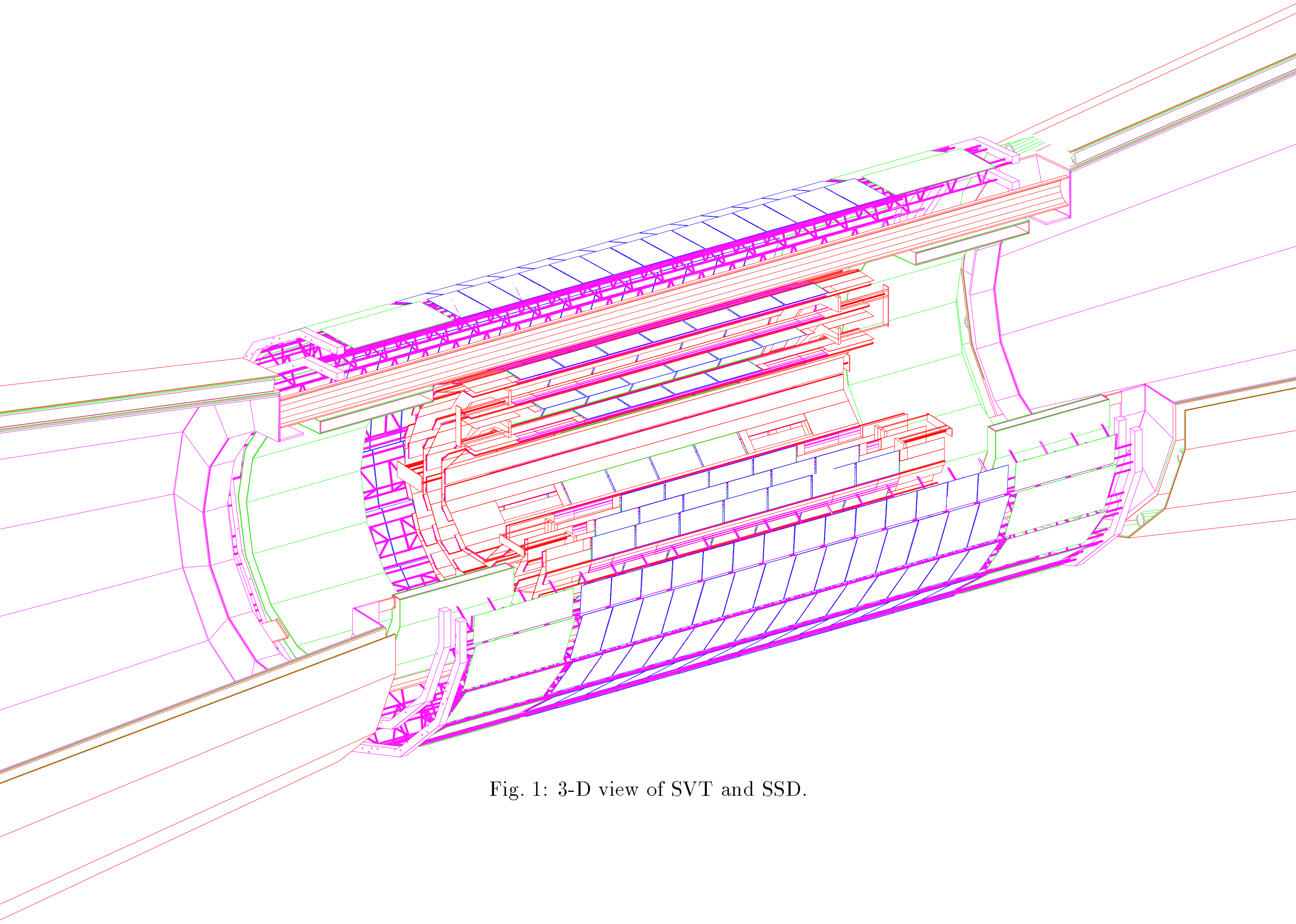

Fig. 1: 3-D view of SVT and SSD.

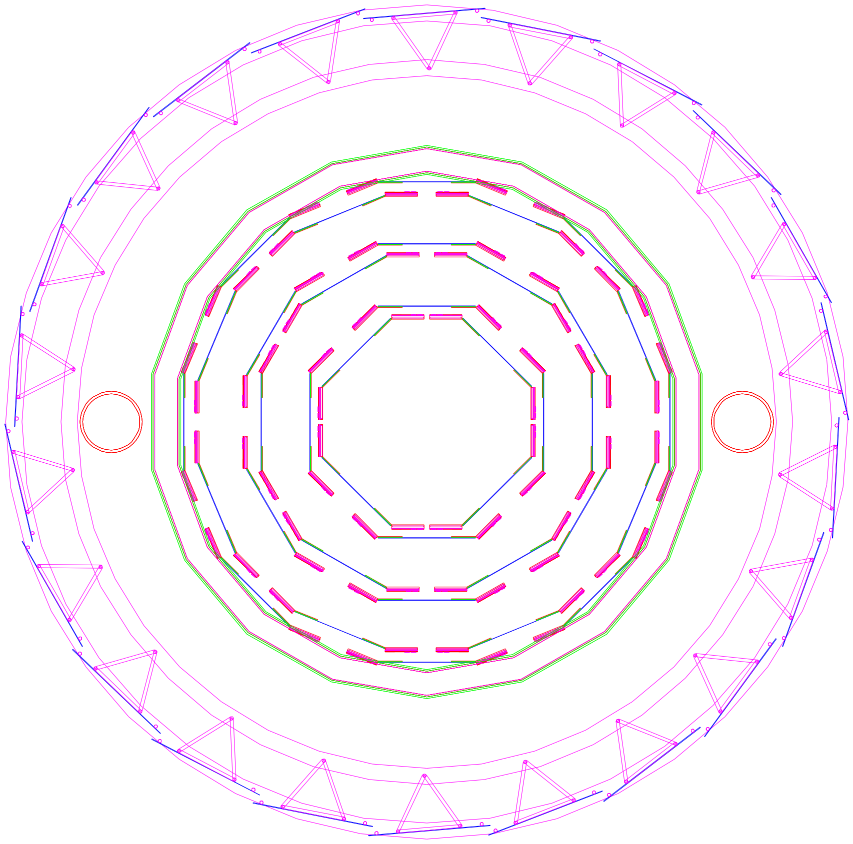

Fig. 2: Endcap view of the proposed SSD implementation.

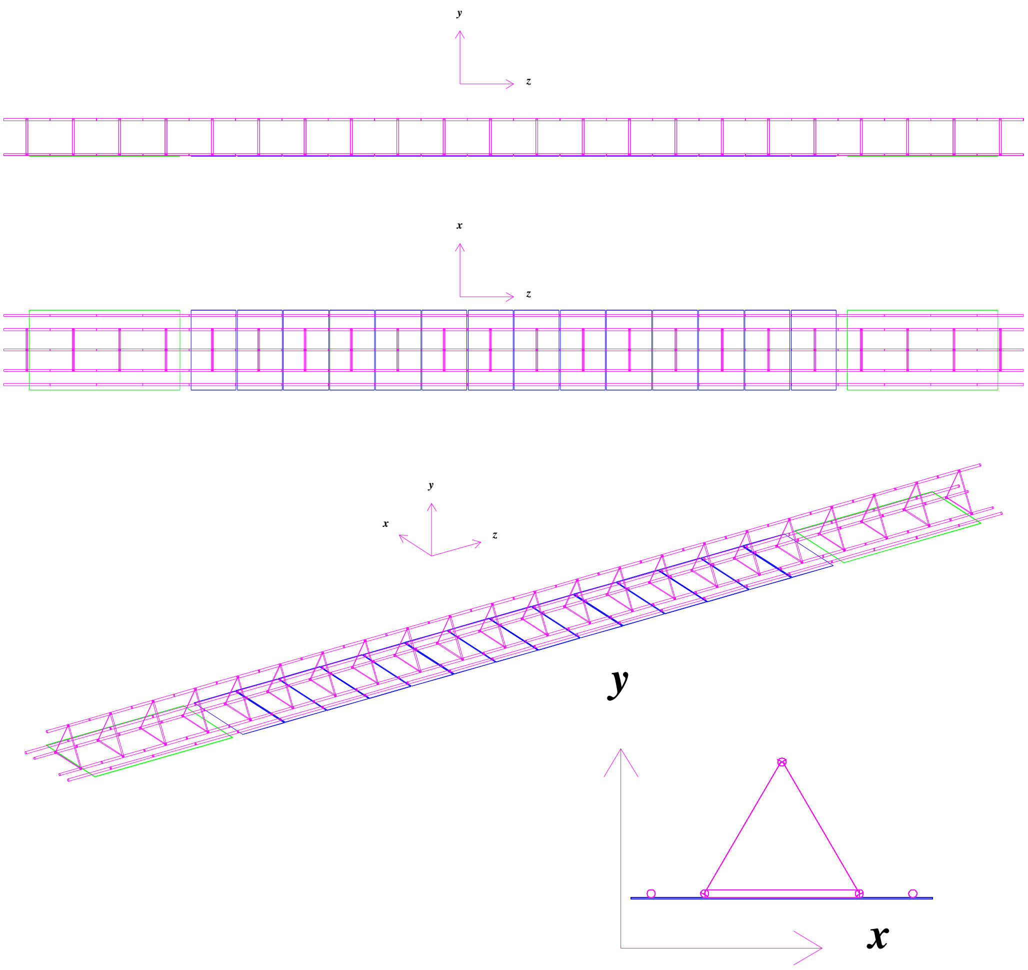

Fig. 3: Details of the SSD support structure. The water channels and the carbon fiber structure can be seen.

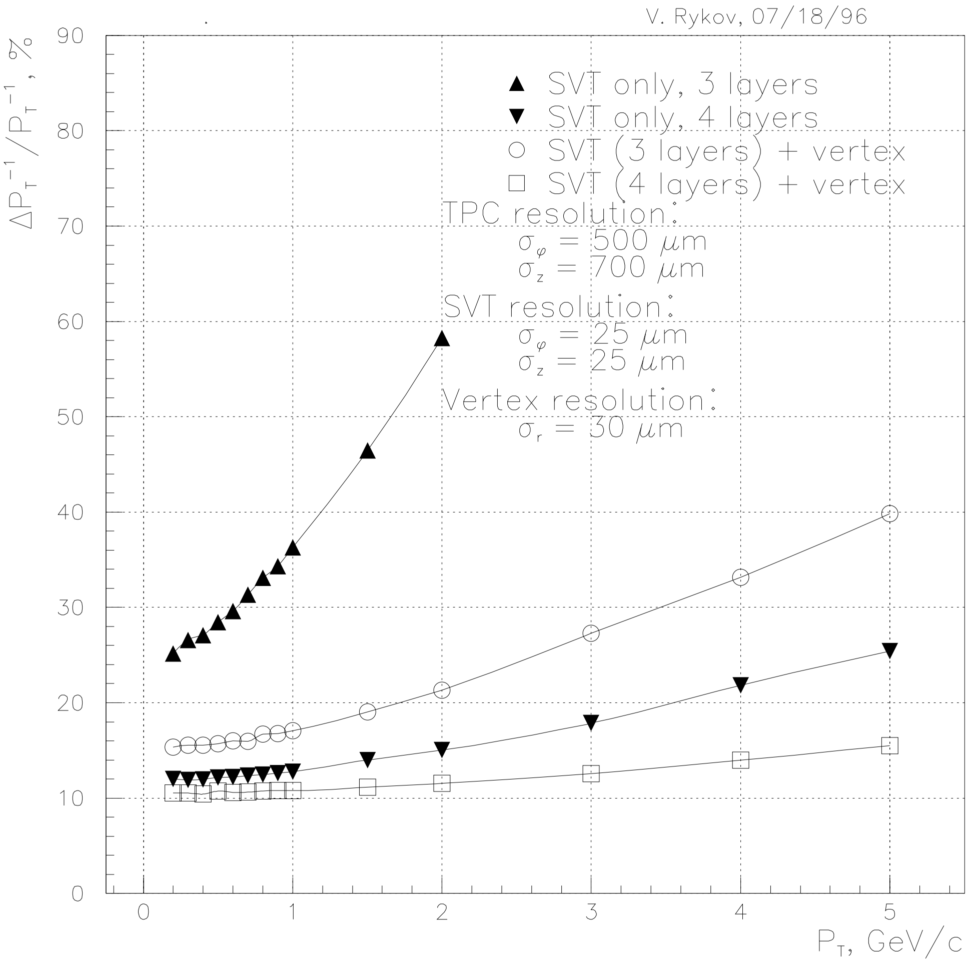

Fig. 4: Improvement in SVT momentum resolution due to the SSD.

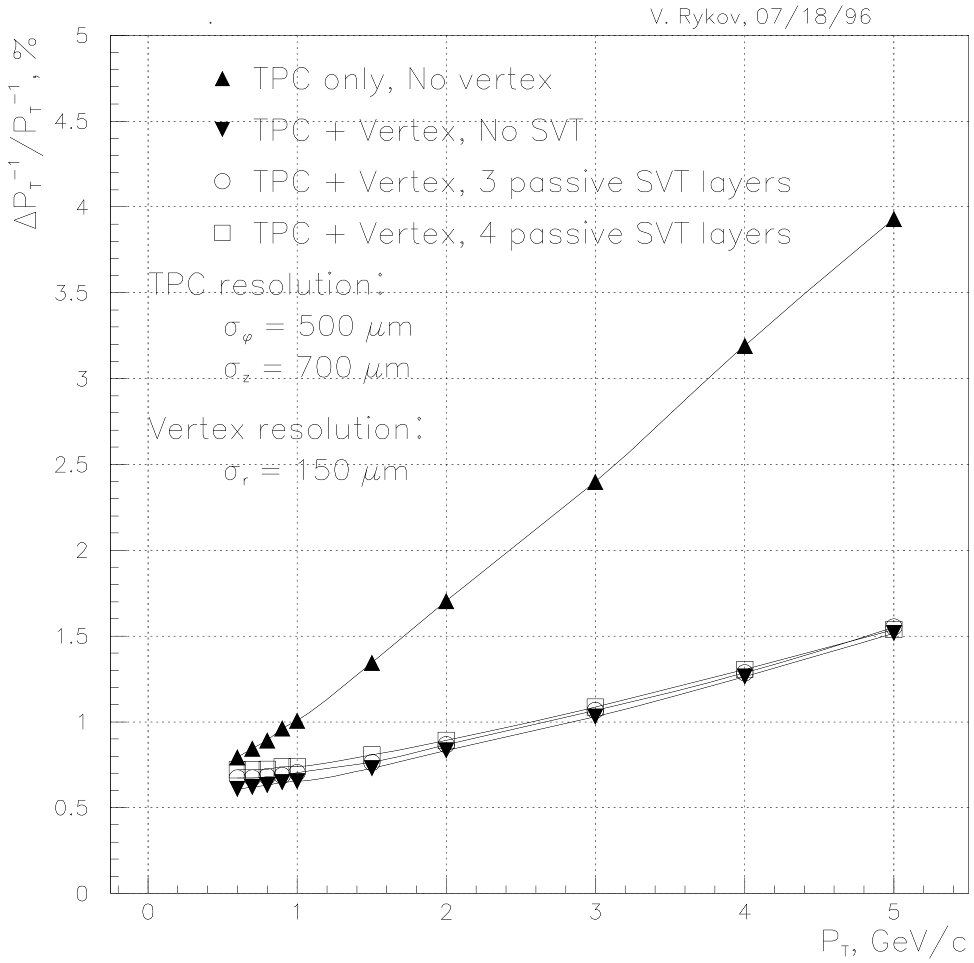

Fig. 5: Effect of the SSD implementation on the TPC momentum resolution.

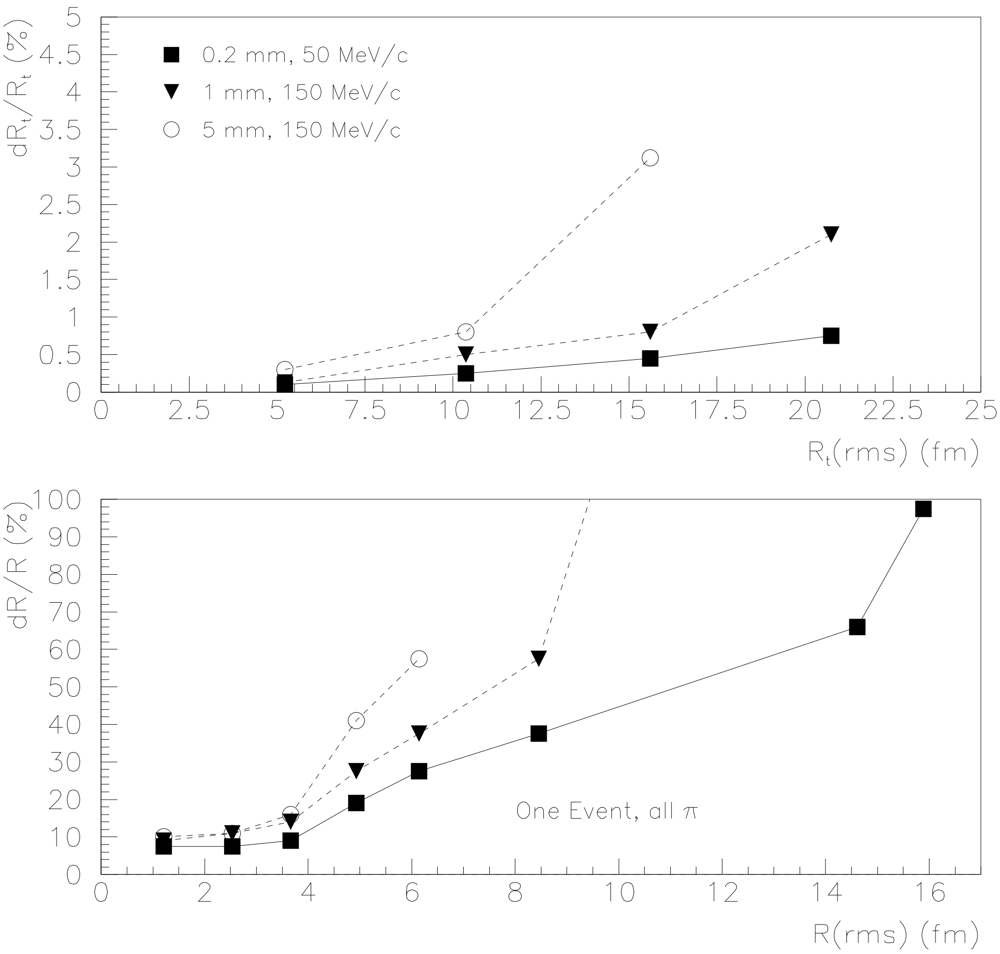

Fig. 6: a.) Uncertainty in rms radius for inclusive pion pair spectra as a function of lower momentum cutoff and two track separation at the outer radius of the SVT. Dashed curves reflect a range for the TPC performance depending on the drift gas, the solid curve is the result of the SVT analysis b.) Same as a.) for single event pion pair spectra.

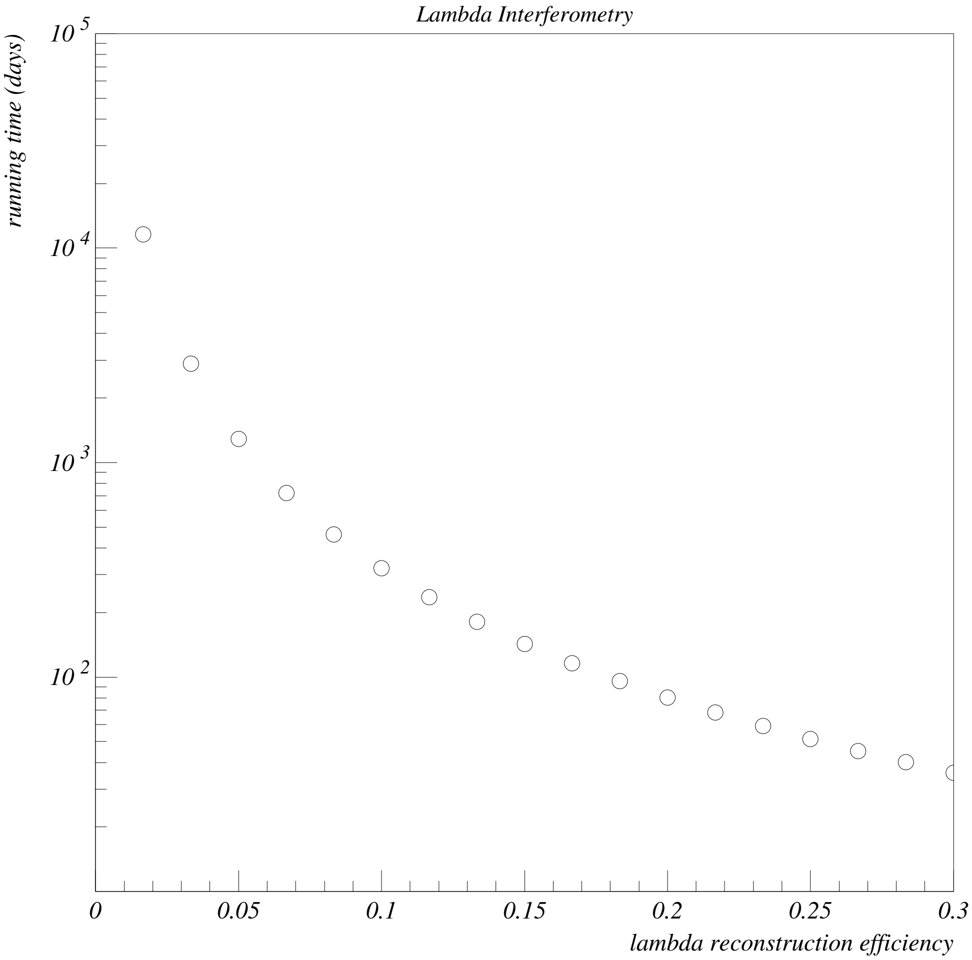

Fig. 7: Central Au-Au running time to reconstruct 5 Million Λ pairs at 1 Hz event rate as a function of Λ reconstruction efficiency in STAR. With the addition of the SSD we expect to achieve an efficiency of about 15%.